THE ANNALS OF "DUNĂREA DE JOS" UNIVERSITY OF GALAȚI
FASCICLE V, TECHNOLOGIES IN MACHINE BUILDING,
ISSN 1221- 4566, 2009

NEWTECH 2009, GALATI

TOOL DEFLECTION ON PERIPHERAL MILLING

Campa, F.J., López de Lacalle, L.N., Lamikiz, A., Bilbao, E., Calleja, A., Peñafiel, J.

University of the Basque Country, UPV/EHU. Faculty of Engineering, Bilbao, Spain
email: fran.campa@ehu.es

ABSTRACT

In this work a mechanistic model for peripheral milling is presented, taking into account the flexibility of slender end mills. The contribution of this paper is the obtention of the real tool center displacements and the real cutting forces, since the model takes into account the instantaneous force balance between the cutting forces and the elastic force of the slender tool.
A deep explanation of the model, some application examples and discussion of the results are in the paper.

KEYWORDS: milling, modelling, tool deflections.

1. INTRODUCTION

The geometrical error caused by tool deflection in peripheral milling is a common problem in the industry. This fact has lead to the development of models to predict the surface and geometrical errors by different researchers in the recent years. In 1991, Montgomery and Altintas [1] considered the influence of milling dynamics on surface generation. In [3,5,8], a geometric model of the machined surface is developed and used to predict its appearance and roughness by considering the sweep volumes by the cutting edges in their paths and subtracting them from the workpiece.

In this paper, a model for the prediction of the tool deflection in peripheral milling taking into account the tool static stiffness is developed. First, the mechanistic forces model is presented. Later, the procedure followed to obtain the deflections is explained. Finally, the model is validated through the comparison of the displacements and forces predicted by the model with the experimental ones.

This model can be easily extrapolated to other tool geometries, adapting the equations of the mechanistic model. The final purpose is the obtention of theoretical topographies based on the tool deflections calculated [2].

2. NOMENCLATURE

a_e: Radial depth of cut (mm)
a_p: Axial depth of cut (mm)
f_z: Feed per tooth (mm)
f: Feed speed (mm/min)
D: Diameter of the tool (mm)
Z: Number of flutes of a tool
N: Spindle speed (rpm)
k_t, k_r, k_a: Tangential, radial and axial shearing cutting coefficient (N/mm^2)
k_x, k_y: Static stiffness in X and Y direction
α: Runout angle
r: Runout

3. TOOL DEFLECTION MODEL

The model here presented incorporates the effect of tool deflection on the forces model to obtain real forces and tool displacements in peripheral milling at cutting frequencies under the first natural frequency of the tool, that is, when a static behaviour for the tool motion can be assumed. Here, the forces model is first presented, and then the procedure for the calculus of the tool static deflections.

3.1 Cutting forces model

The forces model for an end mill is based on a mechanistic approach [1,4] which discretizes the cutting edge, obtains the forces on each differential element and the integrates the forces to take into account the contribution to the total forces of each element of each cutting edge in cut. The cutting forces model on one differential element takes into account

the shearing forces and the edge forces by means of a tangential, radial and axial component, see Fig. 1.

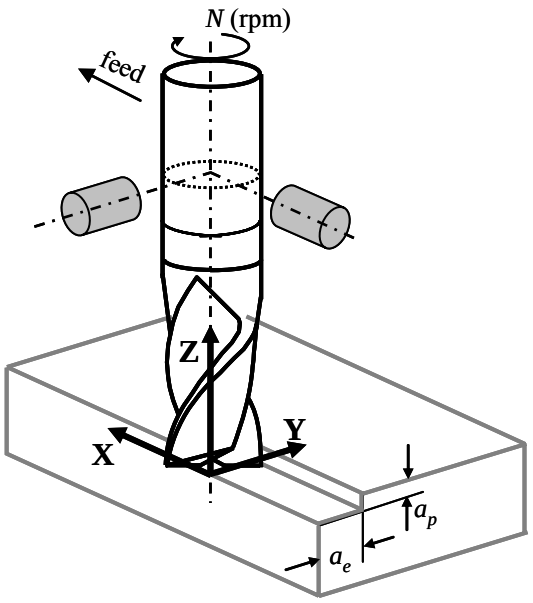

Fig. 1. Schematic representation of the reference system.

These components depend on the correspondent cutting coefficients, the chip thickness *h*, the differential width of cut *db* and the differential edge length *dS*:

$$\begin{aligned} dF_{t,j}\left(\phi_j,\kappa\right) &= K_{te}dS + K_{tc}h\left(\phi_j,\kappa\right)db \\ dF_{r,j}\left(\phi_j,\kappa\right) &= K_{re}dS + K_{rc}h\left(\phi_j,\kappa\right)db \\ dF_{a,j}\left(\phi_j,\kappa\right) &= K_{ae}dS + K_{ac}h\left(\phi_j,\kappa\right)db \end{aligned} \quad (1)$$

The differential width of cut *db* depends on the geometry of the tool as:

$$db = dz / \sin\kappa \quad (2)$$

The angular position of an element of the j^{th} cutting edge is defined as a function of the pitch angle of the tool ϕ_p and the lag angle ψ of the element due to the helix angle with respect to the element of that edge at z=0:

$$\phi_j\left(\phi,z\right) = \phi + \left(j-1\right)\phi_p - \psi\left(z\right) \quad (3)$$

The tangential, radial and axial differential forces are projected over the Cartesian axes, indicated in Fig. 1, by means of a rotation matrix:

$$\left\{dF_{xyz,j}\left(\phi_j,z\right)\right\} = \left[R\right]\left\{dF_{tra,j}\left(\phi_j,z\right)\right\}$$

$$\left[R\right] = \begin{bmatrix} -\cos\phi_j & -\sin\kappa\sin\phi_j & -\cos\kappa\sin\phi_j \\ \sin\phi_j & -\sin\kappa\cos\phi_j & -\cos\kappa\cos\phi_j \\ 0 & \cos\kappa & -\sin\kappa \end{bmatrix} \quad (5)$$

The total cutting forces over the jth edge are calculated by integration, where the limits of integration depend on the angular position of the edge due to the helix angle i_0 [1].

$$F_{xyz,j}\left(\phi_j\right) = \int_{z_1}^{z_2} dF_{xyz,j}\left(\phi_j,z\right) \quad (6)$$

Finallly, the total forces are obtained taking into account the contribution of each edge inside the cutting area:

$$F_{xyz}\left(\phi_j\right) = \sum_{j=1}^{Z} F_{xyz,j}\left(\phi_j\right) \quad (7)$$

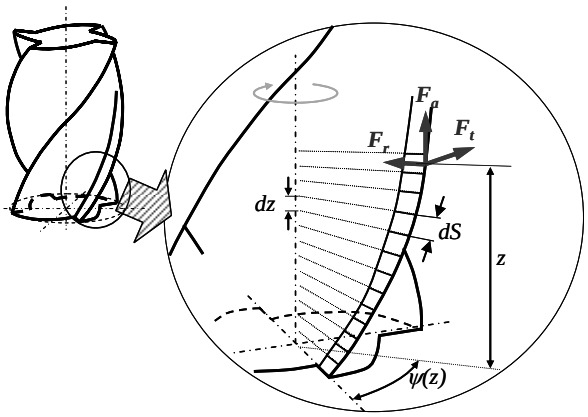

Fig. 2. Schematic representation of the cutting forces and geometrical parameters.

Geometry of the tool and the cutting edge

The integration of the forces depends on the geometry of the tool, which is a function of several geometrical parameters of the tool. Since the procedure to obtain these parameters has been well studied by other authors [4], here it is not demonstrated how to obtain them, so only the necessary equations are shown. In the flank of an end mill, where the helix angle is constant, the height z of an edge element is related to the helix angle, the diameter of the tool *D* and the lag angle ψ as:

$$z = \frac{D/2\cdot\psi}{\tan\left(i_0\right)} \rightarrow \psi = \frac{z\cdot\tan\left(i_0\right)}{D/2} \quad (8)$$

Additional parameters that are needed are the radius of each element,

$$r(z) = R \tag{13}$$

and the corresponding edge lead angle:

$$\kappa(z) = 90^{o} \tag{14}$$

Finally, the differential edge length can be obtained as:

$$dS(z) = dz\sqrt{\left(\left(r'(z)\right)^2 + \left(r(z)\phi_j'\right)^2 + 1\right)} \tag{15}$$

3.2 Static deflections model

Hypotheses

In this work, it is assumed that the tool suffers only static deflections during the milling. This assumption is supposed to work when the cutting frequencies are lower than the first natural frequency of the tool to keep a low dynamic amplification and a phase between forces and displacements near to 0º. In that range of cutting frequencies, the stiffness of the tool is approximately the static one.

Hence, it can be supposed that the tool rotates at an infinitely low spindle speed and as a consequence, at each position, the tool deflects to a position where there is a balance between the cutting forces and the elastic forces of the tool. In the equation of the motion of the tool the terms of damping and inertia are thus neglected:

$$\begin{bmatrix} k_{xx} & k_{xy} \\ k_{yx} & k_{yy} \end{bmatrix} \begin{Bmatrix} x(t) \\ y(t) \end{Bmatrix} = \begin{Bmatrix} F_x\left(x(t), x(t-T)\right) \\ F_y\left(y(t), y(t-T)\right) \end{Bmatrix} \tag{16}$$

As it can be seen only the tool deflections in the XY plane have been considered.

It is also assumed that the tool has the same stiffness along the cutting edge, which is valid for relatively low depths of cut.

Iterative algorithm

Although Eq. 16 is apparently a simple equation to solve, the fact is that the relation between cutting forces and displacements is not explicit. In Eq. 1, it can be seen that the forces depend on the chip thickness, which depends on the displacements of the tool and the tool runout *r*:

$$h = \left(f_z \sin\phi + r\cos\alpha + \Delta x \sin\phi + \Delta y \cos\phi\right)\sin\kappa \tag{17}$$

Where the displacements take into account the deflection on the previous tooth engagement:

$$\begin{aligned} \Delta x &= x(t) - x(t-T) \\ \Delta y &= y(t) - y(t-T) \end{aligned} \tag{18}$$

Hence, to obtain the static deflections, the following iterative procedure has been programmed:

First, for a given tool geometry and a set of cutting parameters, the total cutting forces F_x, F_y, F_z are obtained at an initial angular position ϕ. These forces are calculated assuming that the TCP is in x=0, y=0.

The deflection caused by these forces is obtained as:

$$x' = \frac{F_x}{k_x};\quad y' = \frac{F_y}{k_y} \tag{19}$$

In a flexible tool, the cutting forces generate a displacement of the tool which changes the real chip thickness affecting again the cutting forces. Only when the displacements generated are similar to the ones used to calculate the forces, it can be said that there is a balance between the cutting force and the elastic force of the tool, and the displacements and forces obtained are realistic.

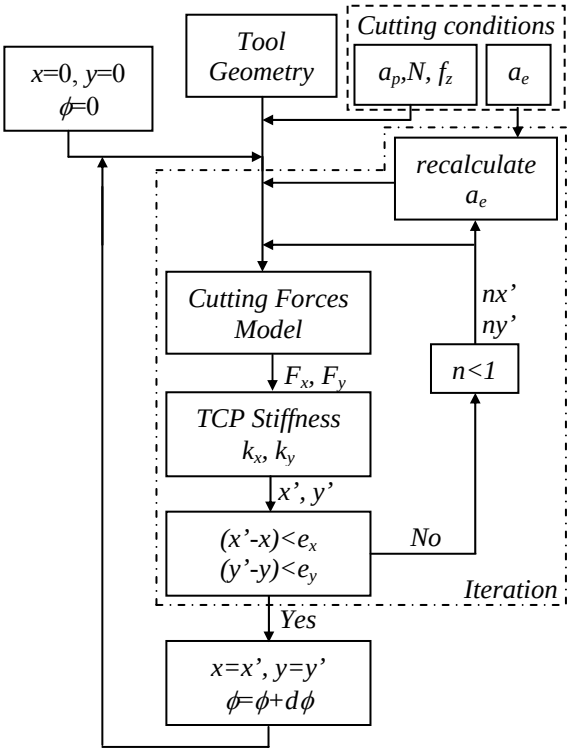

Fig. 3. Iterative procedure for the obtention of the static deflections in the TCP.

Hence, if the difference between the initial TCP position (x,y) and the TCP obtained (x',y') is lower than a threshold value (e_x,e_y), the calculation of the deflection for the next angular position is started. If not, the new position is fed back to calculate new forces until the difference of positions x-x' and y-y' is lower than the threshold value. The magnitude of the

threshold values determines the accuracy of the calculation. Also, it is needed to recalculate the radial depth of cut as it is affected by the displacement in Y direction. Finally, to ensure the convergence of the algorithm, the displacements fed back are multiplied by a factor lower than 1. The higher the factor, the faster the calculus, although it rises the risk of convergence problems. Fig. 3 summarizes the proposed procedure.

3.3 Comparison rigid tool-flexible tool

To study the influence of the tool flexibility, the forces and displacements for a flexible tool and a rigid tool under the same cutting conditions have been calculated and compared. The cutting conditions are down-milling, axial depth of cut 8 mm, radial depth of cut of 3 mm, feed per tooth 0,05 mm, and an end mill of 16 mm of diameter, 2 cutting edges and 30º of helix angle.

Figure 4 shows the comparison between the forces in an infinitely rigid tool and a flexible tool. While the forces in the stiff tool remain always the same, the forces on the flexible tool are initially lower, since the tool cuts less material than the imposed due to the deflection. However, the machine tool imposes a feed per revolution, so the tool is finally carried by the machine, and in the following revolutions it cuts the stock of material that was not initially cut. It can be seen in the Fig. 4 how after the first revolution, the forces increase due to the stock removal, and then they stabilize to a value similar to the forces in the rigid tool.

The explanation for this behaviour can be found in the balance between the cutting forces that deflect the tool and the elastic forces of the tool that counteract the deflection. When this balance is reached in a flexible tool, the cutting forces are the same as in a rigid tool. However, while the rigid tool remains immovable, the flexible tool deflects. In fact, in the Fig. 5 it can be seen how the displacements of the tool increase also until they stabilize.

Regarding the algorithm, for very low tool stiffnesses and agressive cutting conditions, the algorithm has problems of convergence. Nevertheless, those cutting conditions are usually unreal. For usual cutting conditions the convergence of the algorithm is faster as the stiffness of the tool is higher. The explanation is that the behaviour of a very flexible tool differs too much from the one of a rigid tool; hence, to find the balance between the elastic forces and the cutting forces, a higher number of iterations are needed.

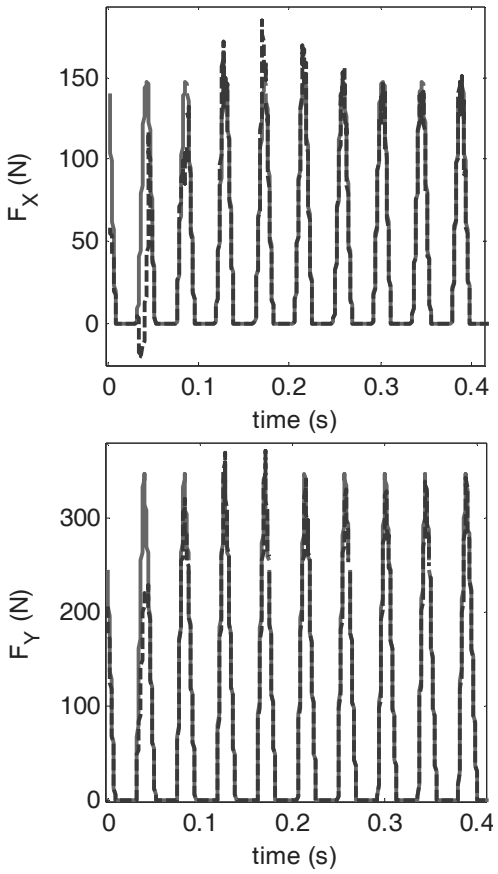

Fig. 4. Cutting forces in X and Y direction: Flexible tool (dashed line) and rigid tool (solid line).

For the cases where the convergence of the algorithm fails, it will be interesting for future works to study if it is possible to experimentally find a static unstability in the tool behaviour, or if this unstability only occurs in the algorithm, or if other phenomenons as regenerative chatter predominate, before the static unstability appearance.

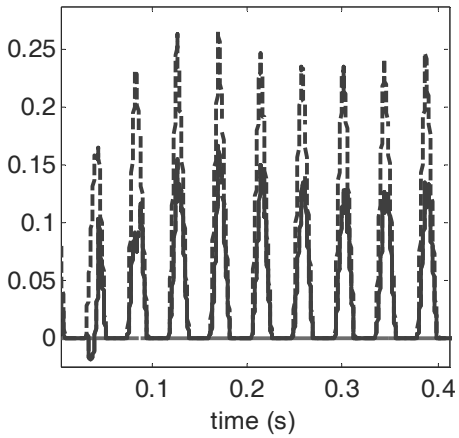

Fig. 5. Tool displacements: in X direction (solid line), in Y direction (dashed line).

3. EXPERIMENTAL VALIDATION

The model has been validated by means of several cutting tests on a five-axis milling machine with a workpiece of Aluminum 7075-T6. The tool is an end mill with a diameter of 16 mm, two cutting edges, 30º of helix angle and an overhang of 105 mm. The tool runout was measured, resulting in an eccentricity of 0,04 mm where the maximum eccentricity was at an angle of 110º with respect to the cutting edge taken as a reference. The cutting coefficients of the tool and material pair are k_{tc}=870N/mm^2, k_{rc}=62 N/mm^2, k_{ac}=60 N/mm^2, k_{te}=12 N/mm, k_{re}=20 N/mm and k_{ae}=0 N/mm. The tests were performed at very low cutting frequencies, 690 rpm, to avoid dynamic effects. Four tests were done with a radial depth of cut of 0,5 and 1 mm, in down-milling. The axial depth of cut was 8,8 mm, and the feed speed was 250 mm/min and 500 mm/min.

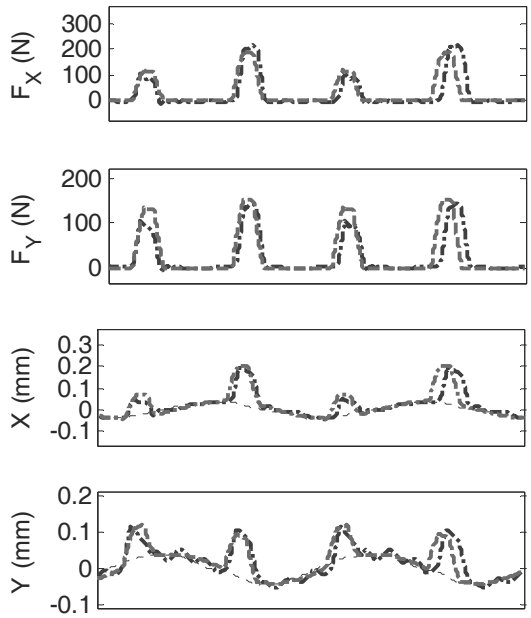

Fig. 6. Forces and displacements for test 1: a_e=0,5mm, v_f=250mm/min.

The tool displacements in X and Y direction during the cutting process were measured at the tool shank using two Eddy-current displacement sensors located at 46 mm from the tool nose. These displacements were later extrapolated to the tool nose measuring the stiffness ratio between the two points. On the other hand, the cutting forces were measured by means of a dynamometric table capable of measuring forces in X, Y and Z direction. The force and displacement signal were recorded by means of a signal analyzer at a sampling frequency of 16384 Hz, and were later low-pass filtered at a cutting frequency of 300Hz.

The measurement of the static stiffness is made by pushing the tool nose against the dynamometric table in X and Y direction. Imposing a known displacement of the tool onto the table of 0,1 mm and measuring the force registered, the static stiffness can be obtained. The stiffness measured at the tool nose was k_x= 1105 N/m and k_y=1380 N/m, and, at 46mm, k_x=2806 N/m and k_y=3505 N/m. Bearing in mind that the tool is axisymmetrical, the asymmetry between k_x and k_y appears to be extrange. However, it must be reminded that the tool only a part of the whole stiffness chain tool-toolholder-spindle-machine, where the machine, which is not axisymmetrical with respect to the tool axis, plays an important role [7].

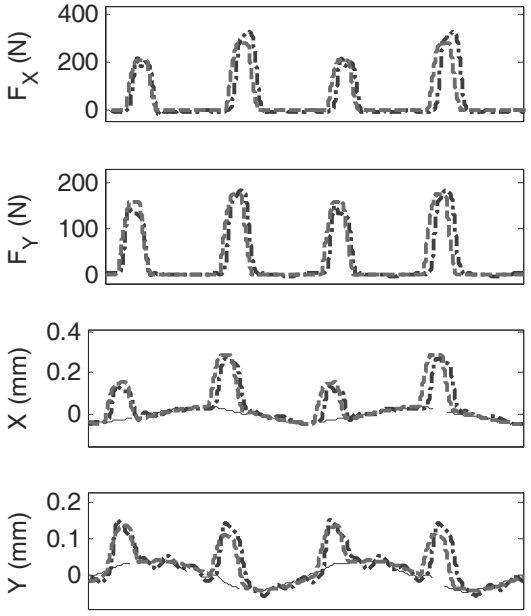

Fig. 7. Forces and displacements for test 2: a_e=0,5mm, v_f=500mm/min.

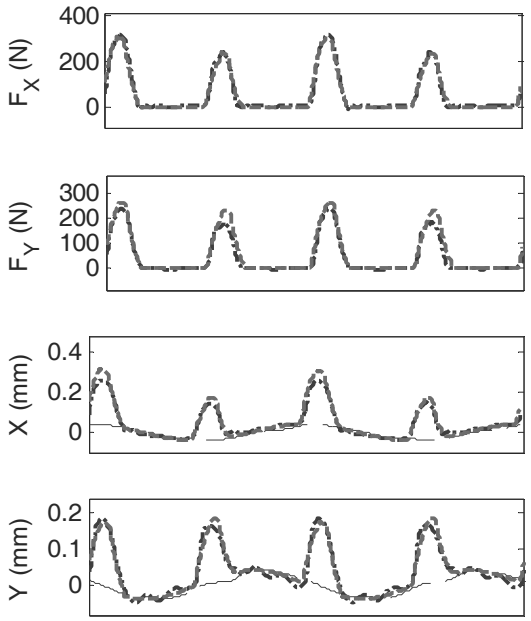

Fig. 8. Forces and displacements for test 3: a_e=1mm, v_f=250mm/min.

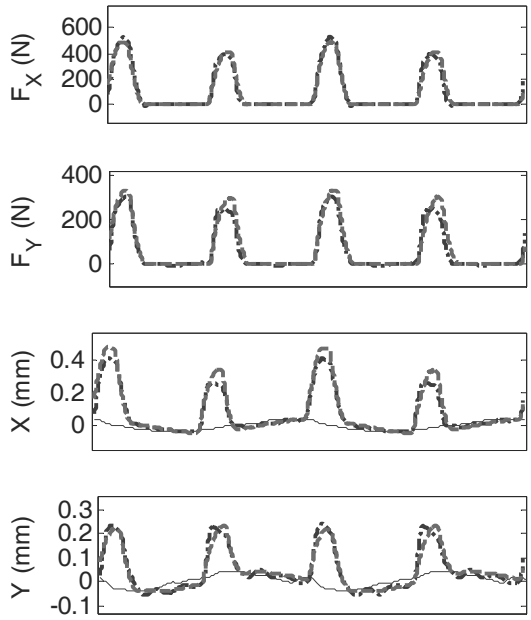

Fig. 9. Forces and displacements for test 4: a_e=1mm, v_f=500mm/min.

The comparison between the forces and displacements measured and the ones calculated is shown in Figs. 6 to 9. The dashed thick line represents the calculated forces and displacements, the dashed dot thick line represents the measured forces and displacements, and the thin line in the displacements represents the tool displacements due to the tool runout before the cutting. The simulations made for comparison took into account the first 5 revolutions of the tool, as the evolution of the forces stabilized fastly. The time required for the calculations was of 214 seconds in Matlab 7, with a CPU with an Intel Celeron at 1,73 GHz and 2,00 GB of RAM.

In the tests shown, the experimental measurements match reasonably well the predictions of the model. These tests have been made at a main cutting frequency of 23 Hz, though, almost 20 times lower than the measured natural frequency of the tool, 458 Hz. The validity of the model has been proved but only in the range of static behaviour of the tool, where the model is expected to work. Hence, the model should fail to predict the tool deflection cutting near the natural frequency of the tool. Nevertheless, the assumption of static behaviour can be assumed in a lot of industrial cases, milling low machinability materials, hard materials, or even in micro milling.

4. CONCLUSIONS

The main contribution of this work is the development of an iterative model for the tool static deflection obtention based on the instantaneous force balance between the cutting forces and the elastic force of the slender tool. The model predicts the static deflection by means of a feedback of the displacements obtained by the cutting forces model into the chip thickness model.

The model predicts that although in the initial revolution a flexible tool deflects cutting less than the feed per tooth, the tool finally always ends following the feed imposed by the machine-tool, hence the cutting forces are similar to a rigid tool. This has been explained by the balance that appears when the elastic forces counteract the deflection caused by the cutting forces.

The algorithm has proved to be reliable and due to the feedback performed, it only has problems of convergence in aggressive yet unreal cutting conditions.

The experimental validation shows that the displacements and forces predicted by the model are reliable whenever the cutting frequencies are much lower than the first natural frequency, and a static behaviour can be assumed.

ACKNOWLEDGEMENTS

The authors would like to thank the Basque Government for supporting this work made under the CRC marGUNE framework.

REFERENCES

[1] Altintas, Y., *Manufacturing Automation,* Cambridge University Press, Cambridge, MA, 2000;

[2] Arizmendi, M., Campa, F.J., Fernández, J., López de Lacalle, L.N., Gil, A., Bilbao, E., Veiga, F., Lamikiz A., *Model for surface topography prediction in peripheral milling considering tool vibration,* CIRP Annals - Manufacturing Technology, 58/1, 2009, pag. 93-96.

[3] Arizmendi, M., Fernández, J., López de Lacalle, L. N., Lamikiz, A., Gil, A., Sánchez, J. A., Campa, F. J., Veiga, F., *Model development for the prediction of surface topography generated by ball-end mills taking into account the tool parallel axis offset. Experimental validation,* CIRP Annals - Manufacturing Technology, 57/1, 2008, pag. 101–104;

[4] Engin, S., Altintas, Y., *Mechanics and dynamics of general milling cutter. Part I: helical end mills,* International Journal of Machine Tools and Manufacture, 41, 2001, pag. 2195-2212;

[5] Jiang H., Long X., Meng G., *Study of the Correlation between Surface Generation and Cutting vibrations in Peripheral Milling,* Journal of Materials Processing Technology, 208, 2008, pag. 229-238;

[6] Montgomery, D., Altintas, Y., *Mechanism of Cutting Force and Surface Generation in Dynamic Milling,* Trans. ASME, Journal of Engineering for Industry, 113, 1991, pag. 160-168;

[7] Salgado, M.A., López de Lacalle, L.N., Lamikiz, A., Muñoa, J., Sánchez, J.A., Evaluation of the Stiffness Chain on the Deflection of End-Mills under Cutting Forces, International Journal of Machine Tools & Manufacture, 45, 2005, pp. 727-739;

[8] Surmann, T., Biermann, D., *The Effect of Tool Vibrations on the Flank Surface Created by Peripheral Milling*, CIRP Annals-Manufacturing Technology, 57/1, 2008, pag. 375-378.